Effects of the 3- and 4-Methoxy and Acetamide Substituents and Solvent Environment on the Electronic Properties of N-Substituted 1,8-Naphthalimide Derivatives

J. L. Gu. Coronado,[†] E. Martín,[†] L. A. Montero,[‡] J. L. G. Fierro,[§] and J. M. García de la Vega*,[†]

Departamento de Química Física Aplicada, Facultad de Ciencias, Universidad Autónoma de Madrid, Cantoblanco, 28049 Madrid, Spain, Laboratorio de Química Computacional y Teórica, Facultad de Química, Universidad de la Habana, La Habana 10400, Cuba, and Instituto de Catálisis y Petroquímica, Consejo Superior de Investigaciones Científicas (ICP-CSIC), Cantoblanco, 28049 Madrid, Spain

Received: July 9, 2007

The photophysical properties of polar molecules in solution with an intramolecular charge-transfer effect in the excited state depend strongly on the polarity and proticity of the solvents. UV−visible spectra of 1,8-naphthalimide and some N-substituted derivatives in acetic acid, acetonitrile, dichloromethane, and *p*-dioxane were carried out. Several molecular cluster geometries formed with N-substituted 1,8-naphthalimide derivatives and a large set of random positioning of some solvent molecules in their environment were optimized by a semiempirical method. It provided a complete screening of possible solute−solvent configurations and resulted in a multiple minima hypersurface of the supramolecular systems. With such local minima energies, the main thermodynamic association functions were found. They also provided selected cluster geometries for calculations of vertical electronic transitions with a time-dependent density functional theory (TD-DFT), if the lowest energy structures were considered. Calculated vertical electronic transition energies at the TD-DFT level were compared with experimental data. The experimental absorption UV−visible spectra for the six compounds in the four solvents were performed in our laboratory. Moreover, X-ray photoelectron spectroscopy of the 1,8-naphthalimide was carried out in the ICP−CSIC laboratory. Thermodynamic function values show different association energies between each solvent and the molecules, in correlation with the possibility of hydrogen bond formation and the polarity and dielectric constant of the solvents. The 3- and 4-acetamide 1,8-naphthalimide derivatives have the highest conformer number and the most negative Gibbs free association energy values for a determined solvent. This indicates the importance of the entropic factors.

Introduction

1,8-Naphthalimide derivatives (Figure 1) have interesting properties to extend their use as tunable dye lasers,[1,2] polymerizable materials,[3,4] fluorescent chemical sensors[5−8] and electroluminescent organic diodes in thin films.[9,10] On the other hand, the 3-amino 1,8-naphthalimide and N-substituted 1,8-naphthalimide derivatives with amino an alkyl side chain linked to the imidic nitrogen have important applications as antitumor agents.[11−14] Their photophysical properties in solutions depend on the polarity and the ability to form a hydrogen bond with the solvents, which generates the solvent-cage environment of the solute molecules.

In previous works,[2,15−18] we have analyzed the experimental electronic properties of some N-substituted 1,8-naphthalimide derivatives in different solvents, such as acetonitrile (MeCN), water, alcohols, *p*-dioxane (*p*-diox), and dichloromethane (DCM). The absorption and fluorescence maxima of the molecules have a red shift with increasing the value of the dielectric constant of the solvents for the derivatives substituted in the 4 position of the naphthalic ring; this red shift is lower for derivatives substituted in the 3 position of the same ring. Usually, we consider that these facts take place in polar molecules that preferably have $\pi-\pi^*$ electronic transitions and dipolar moments in the Frank Condon excited state S_1 higher that those in the ground state S_0.

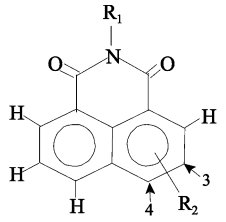

Molecule	R_1	R_2
1	-H	-H
2	$-(CH_2)_2-N(CH_3)_2$	$-NH-COCH_3(3)$
3	$-(CH_2)_2-N(CH_3)_2$	$-NH-COCH_3(4)$
4	$-(CH_2)_2-N(CH_2)_4$	$-OCH_3(3)$
5	$-(CH_2)_2-N(CH_2)_4$	$-OCH_3(4)$
6	$-CH_2-CH_3$	$-OCH_3(4)$

Figure 1. Structure of 1,8-naphthalimide and its derivatives.

When electron donor groups at positions 3 or 4 in the naphthalene ring (amine, methoxy, or acetamide) are introduced, the lowest singlet excited state of the 1,8-naphthalimide is modified. The derivatives substituted in position 3 have a new absorption band in the visible zone, around 415, 375, and 380 nm for amino, methoxy, and acetamide groups, respectively. However, the derivatives in position 4 have the specific band

* To whom correspondence should be addressed. Tel: +34-91-4974963. Fax: +34-91-4974512. E-mail: garcia.delavega@uam.es.
[†] Universidad Autónoma de Madrid.
[‡] Universidad de la Habana.
[§] Consejo Superior de Investigaciones Científicas (ICP-CSIC).

10.1021/jp075336a CCC: $37.00 © 2007 American Chemical Society
Published on Web 09/07/2007

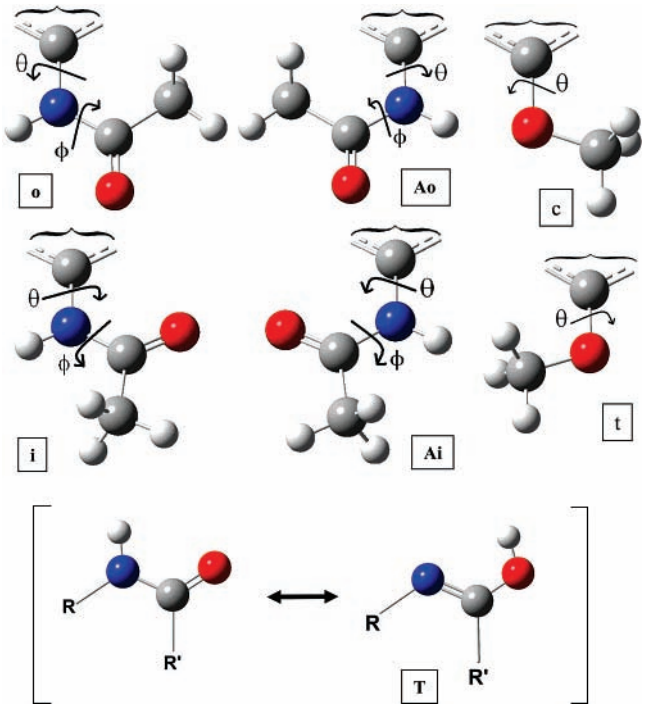

Figure 2. Denomination of possible isomers; rotational conformers of −NHCOMe (out and in, asymmetric out and asymmetric in) and of −OMe (trans and cis). Tautomerism imide−imidol.

of 1,8-naphthalimide, without vibrational structure and broadness, red shifted approximately 30 and 35 nm for the methoxy and acetamide groups, respectively.

The photophysical properties (fluorescence, lifetime, and fluorescence quantum yield) increase to a higher degree at position 4 than they do at position 3. The substituted compounds at position 4 show a clear electronic donor character for the carboxyimide group and favor the radiative deactivation of the excited state of the molecules using the laser emission by excitation with nitrogen or Nd:YAG lasers.[2,19] Nevertheless, the derivatives substituted in position 3 have very low fluorescence, and their lifetime appears in the picosecond range. An intramolecular charge transfer (ICT) occurs when the imide nitrogen is linked to the ethyl with an amino terminal group in R_1. For this reason, the fluorescence emission for all derivatives is quenched, and the absorption properties are slightly modified. The addition of acetic acid (AcH) to the solution eliminates the ICT effect by the protonation of the amino nitrogen in R_1. Similar effects have been reported by other authors, such as PET (photoinduced electron transfer).[20−22]

Some calculations on these molecules have been carried out in the gas phase.[18,21−23] A high degree of coplanarity and charge transfer between the π system of the naphthalene ring and the carboxyimide group in the reference molecule 1,8-naphthalimide is shown. The aliphatic chain linked to the imidic nitrogen modifies both the coplanarity of the chromophore and, very slightly, the electronic fundamental transition. The substitution by donor groups in the 3 or 4 position of the naphthalic ring generates new theoretical vertical transitions, which agree partially with a few spectra.

The aim of this work is to study the influences of the R_1 and R_2 substituents and the solvents on the photophysical properties. Systematic studies of 1,8-naphthalimide (**1**) and five N-substituted derivatives (**2**−**6**) (see Figure 1) in four solvents, namely, MeCN, *p*-diox, DCM, and AcH, are performed at experimental (UV−visible) and theoretical levels. Moreover, in order to study the 1,8-naphthalimide imidol tautomerism, X-ray photoelectron spectroscopy (XPS) of the solid phase is carried out.

TABLE 1: Calculated ΔH_{as} and ΔG_{as} (kJ/mol at 298K) of the 1,8-Naphthalimide and its Tautomer (1 and 1T) for the Gas Phase and *n* Molecules of the Solvent Phase

		1		1T	
phase	*n*	ΔH_{as}	ΔG_{as}	ΔH_{as}	ΔG_{as}
p-diox	1	−12.4	−17.6	−14.7	−18.9
	2	−10.8	−17.9	−12.5	−19.5
	3	−10.5	−17.6	−12.0	−18.3
AcH	1	−21.9	−24.8	−23.9	−26.9
	2	−17.0	−23.2	−20.2	−26.6
	3	−16.6	−23.9	−20.2	−26.7
DCM	1	−10.4	−14.9	−12.0	−15.2
	2	−8.6	−14.8	−10.4	−16.4
	3	−7.9	−15.4	−9.9	−16.5
MeCN	1	−9.0	−12.3	−14.0	−16.2
	2	−8.5	−15.0	−11.1	−16.6
	3	−8.3	−15.5	−10.2	−16.3

Experimental Methods

Absorption UV−visible spectra were recorded in our laboratory using a Perkin-Elmer Lambda 16 UV−vis double beam spectrophotometer with tungsten−halogen and deuterium sources and with quartz cells 10 mm thick. The spectra of the six molecules were obtained in four solvents with different dipole moments and dielectric constants, respectively, *p*-diox (0D, 2.21), MeCN (3.9D, 36.6), DCM (1.6D, 8.93), and AcH (1.7D, 6.20). All molecules studied were synthesized in pharmacology laboratories and were tested by NMR and FTIR methods. All concentrations of the solutions were approximately. 2.0×10^{-4}−1.0×10^{-5} M, and no aggregation effects were observed.

XPS from the ICP−CSIC laboratory was used for the detection of the 1,8-naphthalimide tautomeric form. Analyses were carried out on a VG Escalab 200R electron spectrometer provided with a Mg/Al Kα double anode X-ray source and a hemispherical electron analyzer. The powder samples pressed in 8 mm diameter copper troughs were fixed on the *XYZ* manipulator. The base pressure in the analysis chamber was maintained below 4×10^{-9} mbar during data acquisition. The area under analysis was around 2.4 mm^2, and the pass energy of the analyzer was set at 50 eV, whose resolution, as measured by the full-width at half-maximum (fwhm) of the $Au4f_{7/2}$ core level, was 1.7 eV. The binding energies were referenced to the C_{1s} peak at 284.9 eV. Data processing was performed with the XPS peak v4.1 program; the spectra were decomposed with the least-squares fitting routine provided with the software by the asymmetrical Gaussian/Lorentzian (90/10) product function after subtracting a Shirley background. Atomic fractions were calculated using peak areas normalized on the basis of sensitivity factors.

Theoretical Background and Computational Details. Figure 1 shows the compounds studied with different functional groups, R_1 linked to the imidic nitrogen and R_2 placed in the 3-(meta) and 4-(para) position on the naphthalic ring. In Figure 2, four possible conformations are considered for the **2** and **3** compounds, two conformations in (i) and out (o) due to rotations of the HN−COMe bond and two conformations antisymmetric in (Ai) and antisymmetric out (Ao) due to rotations of the C−NHCOMe bond and the tautomeric forms in Tautomeric (iT) and out Tautomeric (oT) corresponding to the NH−COMe ↔ N═C(OH)Me possible equilibrium (see Figure 2). When the R_2 is a methoxy group (**4**, **5**, and **6** compounds), two conformations are explored (see Figure 2) for rotational isomers of the

TABLE 2: Theoretical (TD-DFT) Vertical Transitions Using 6-31G* and cc-pVDZ Basis Sets and UV−Vis Absorption Bands of the 1,8-Naphthalimide and Its Tautomer (1 and 1T, respectively) for the Gas Phase and *n* Molecules of the Solvent Phase

		1				**1T**					
		6-31G*		cc-pVDZ		6-31G*		cc-pVDZ		Exp[a]	
phase	*n*	λ (nm)	*f*	λ (nm)	f	λ (nm)	*f*	λ (nm)	*f*	λ (nm)	log ϵ
gas		326	0.172	328	0.166	342	0.175	344	0.168	–	–
		219	0.396	221	0.416	226	0.200	228	0.195		
p-diox	1	326	0.197	328	0.191	341	0.107	341	0.107		
		220	0.389	222	0.410	226	0.201	226	0.201		
	2	327	0.212	329	0.205	343	0.184	344	0.133	330{343}	4.117
		220	0.398	222	0.418	226	0.196	228	0.196	220	4.560
	3	329	0.205	331	0.199	344	0.178	346	0.170		
		221	0.379	223	0.413	227	0.197	229	0.196		
AcH	1	328	0.194	329	0.187	341	0.196	341	0.196		
		221	0.337	223	0.367	226	0.206	226	0.206		
	2	328	0.206	330	0.194	342	0.207	344	0.202	340	4.053
		220	0.338	223	0.414	225	0.106	228	0.173	248	3.333
	3	331	0.186	332	0.180	343	0.157	345	0.199		
		221	0.319	223	0.316	226	0.179	228	0.176		
DCM	1	329	0.176	331	0.171	344	0.203	346	0.198		
		221	0.305	223	0.354	226	0.193	228	0.193		
	2	331	0.175	333	0.169	346	0.201	347	0.194	332{342}	4.115
		222	0.197	224	0.424	227	0.174	228	0.173	236	4.587
	3	332	0.172	334	0.166	348	0.219	350	0.212		
		222	0.304	224	0.413	227	0.162	229	0.161		
MeCN	1	328	0.171	330	0.165	342	0.198	342	0.198		
		221	0.292	223	0.299	226	0.195	226	0.195		
	2	331	0.168	332	0.162	344	0.195	345	0.189	331{343}	4.052
		221	0.306	223	0.428	226	0.170	228	0.175	230{212}	4.612
	3	332	0.172	333	0.167	346	0.215	348	0.210		
		222	0.433	224	0.436	226	0.126	228	0.160		

[a] In the brace {} is a submerged band or a less intense band.

C−OMe bond, cis (c) and trans (t). In Figure 2, we have also depicted the imidol tautomeric form **1T** of the reference compound 1,8-naphthalimide (**1**), which has importance in molecular reactivity.

In order to consider the thermodynamic values related to the association of the compounds (**1**−**6**) and the solvents (*p*-diox, DCM, MeCN, and AcH), the theoretical concepts developed to reproduce the solvent direct interactions among the solute and *n* solvent molecules are summarized elsewhere.[24] Since we are working with cluster formation and chemical equilibrium, some relationships can be obtained.

The association process between a solute and *n* solvent molecules can be described by

$$\mathrm{X} + n(\mathrm{solvent}) \rightarrow \mathrm{X(solvent)}_n \qquad (1)$$

For a simple change in an isolated molecule, one can write, for any intensive thermodynamic function like association enthalpy H and free energy G

$$\Delta H_{\mathrm{as}}^{\mathrm{x}} = \Delta H_{\mathrm{x(solvent)}n} - \Delta H_{\mathrm{x}} - n\Delta H_{\mathrm{solvent}} \qquad (2)$$

$$\Delta G_{\mathrm{as}}^{\mathrm{x}} = \Delta G_{\mathrm{x(solvent)}n} - \Delta G_{\mathrm{x}} - n\Delta G_{\mathrm{solvent}} \qquad (3)$$

The energy of the ensemble in a determined state can be obtained by solving the appropriate Schrödinger equation of each solute−solvent cluster relevant to the macroscopic statistical ensemble.[24] Due to the huge computational effort implicit to this task, our attention will focus on finding a reduced set of cells that can represent the most significant contributions to this state for the whole system. Then, we will use a Boltzmann distribution to calculate the thermally averaged state of the typical macroscopic system at room temperature. In any case, the partition function of molecular association should be calculated by assuming the appropriate energy scale with respect to a reference value. For this purpose, a conventional state has to be chosen for calculating such a reference energy. For instance, we can define such a state to exclude all interaction energies among constituent molecules in a given cluster. This means that we would consider the translational, rotational, and vibrational states of molecules in the clusters as identical to those in the reference states. The association process is then considered to be isothermal. In this case, the reference state is taken as a set with the same number of noninteracting molecules of the same solute and solvent kinds and individually optimized with the same energy surface function as the cluster so that the sum of their total energies is taken as the reference value on our energy scale.

It must be pointed out that the association process described by eq 1 implies the appearance of nonnegligible values of energy corresponding to certain intermolecular degrees of freedom appearing in the solute−solvent cluster. They are those related to the rotational modes of the cluster and the intermolecular modes of vibration. We assume that the neglect of these thermal contributions to the association energy terms will not be important since their expected significance must be small with respect to the main energy values.

A large set of random geometries of molecular clusters with different solvents and gas-phase solutes were optimized with the AM1 Hamiltonian performing the MOPAC v.6 program.[25] Therefore, a complete random screening of possible solvent−solute arrangements was then done, and the multiple minima hypersurface (MMH) of the cluster systems and the corresponding thermodynamic quantities were found after finding the partition function of association of the gradient-optimized initial structures.

A study of the association energy evolution per mole of solvent, corresponding to solvated shells, with an increasing

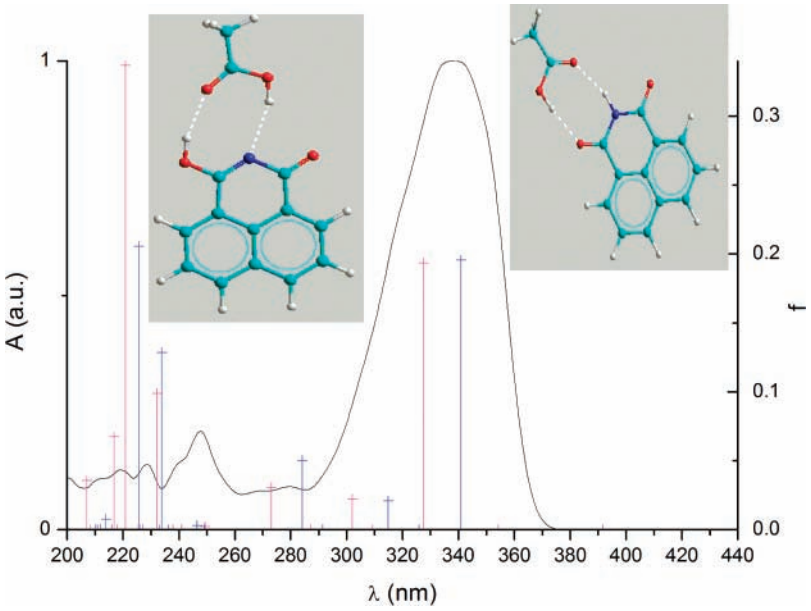

Figure 3. UV−vis absorption spectrum and theoretical vertical transitions for 1,8-naphthalimide (magenta color and right model) and its tautomer (cyan color and left model) in acetic acid solvent (AcH).

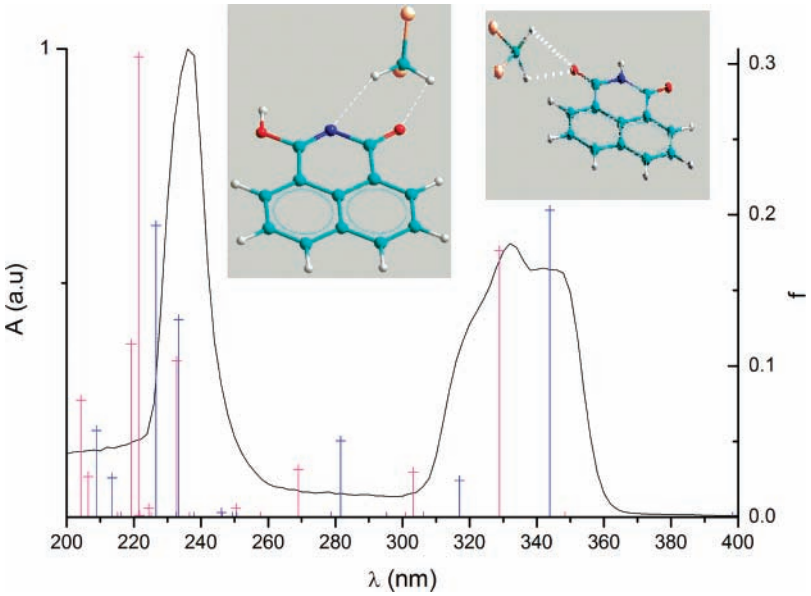

Figure 4. UV−vis absorption spectrum and theoretical vertical transitions for 1,8-naphthalimide (magenta color and right model) and its tautomer (cyan color and left model) in methylene chloride solvent (DCM).

number of solvent molecules was performed. It has been built by taking into account all 25 optimized sets to explore the MMH as described above. It has been reported that the AM1 optimization exaggerates certain solvent−solvent interactions.[26] We found consistency with the procedure of ranking the MMH information for $n - 1$ molecules of solvent and using it in the next calculation of n molecules as a Markov process. Then, the thermodynamic functions of association converge faster, and very similar final energies to those using $n + 1$ molecules of solvent are obtained, which have symmetrical molecular arrangements, making degenerate clusters in MMH.[27]

At this point, three molecules of solvent, as microstates in a canonical statistical ensemble, can represent the main perturbation to these properties with respect to the isolated solute molecule. We have carried out calculations with four and five solvent molecules for molecule **1**, and the thermodynamic properties do not change with respect to the cluster containing three solvent molecules. The space of the nondegenerate microstates to calculate all thermodynamic functions corresponds to 25 optimized clusters per molecule of solvent. The energy of interaction of one molecule of solvent with the solute molecule shows a more important contribution than the addition of more solvent molecules. The more probable minima are found by means of a similarity index (given the nondegenerate states) and a Maxwell−Boltzmann distribution (each microstate with its statistical weight).

By taking into account the geometries of more probable minima of each cluster, vertical excitations and oscillator strengths were calculated with the time-dependent density functional theory (TD−DFT)[28,29] method using the B3LYP functional[30,31] and two basis sets (6-31G* and cc-pVDZ) carried out with a Gaussian program suite.[32] The size of the molecules studied (up to 85 atoms) imposes constraints as to the size of the basis sets that are manageable with the quantum chemical computations. The calculations on compound **1**, carried out also with a more expensive basis set (cc-pVDZ) at the same level

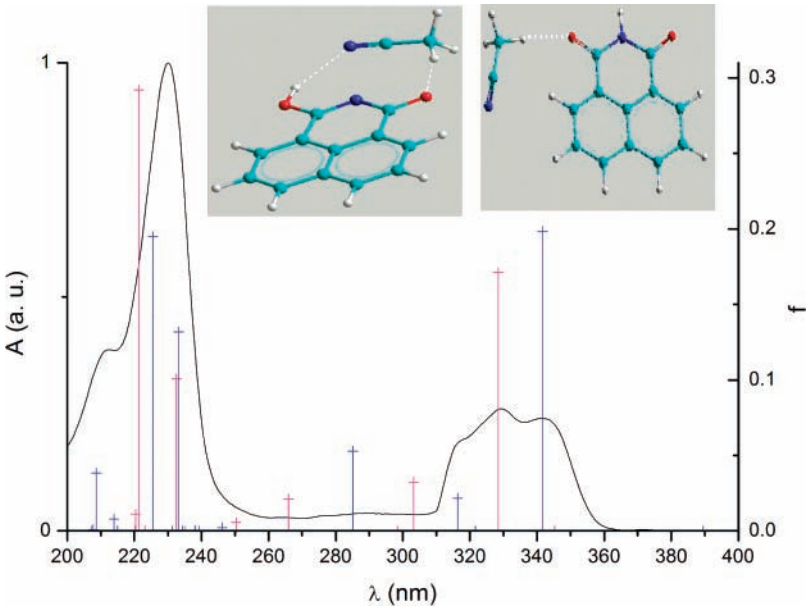

Figure 5. UV−vis absorption spectrum and theoretical vertical transitions for 1,8-naphthalimide (magenta color and right model) and its tautomer (cyan color and left model) in methylene chloride solvent (MeCN).

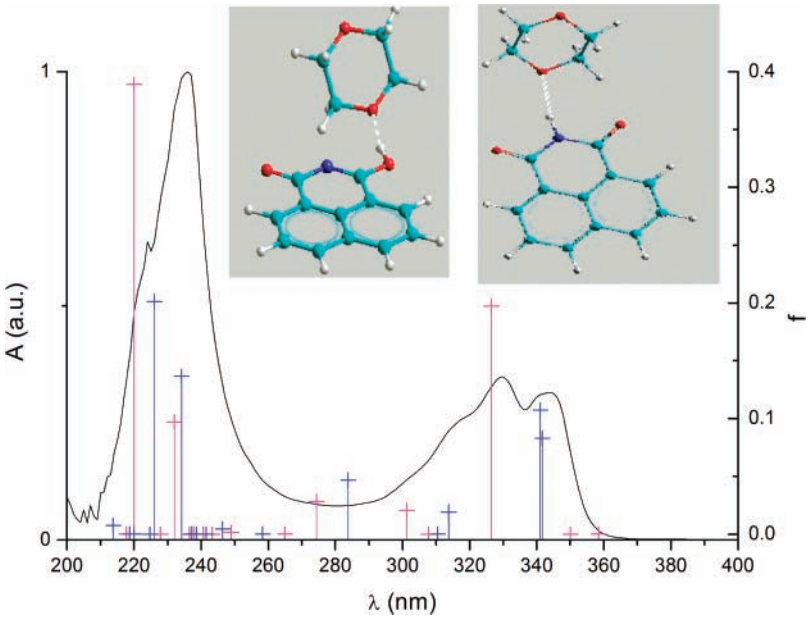

Figure 6. UV−vis absorption spectrum and theoretical vertical transitions for 1,8-naphthalimide (magenta color and right model) and its tautomer (cyan color and left model) in methylene chloride solvent (*p*-diox).

of calculation, will lead to the same values for the vertical excitations. For this reason, the remaining molecules (**2**−**6**) were calculated at the B3LYP/6-31G* level.

Results and Discussion

With the above methodology, we have optimized the corresponding supermolecule of each compound and their tautomers and conformers (**1**−**6**) with one, two, and three molecules of the four solvents plus the six compounds in the gas phase, building a total number of 54 clusters. For each supermolecular structure, we have carried out the thermodynamical and TD-DFT calculations (1350 states). First, we analyzed the results for compound **1**, and we continued with the study of the different derivatives (**2**−**6**).

Effects of the Substituents and the Solvents on the *N*-1,8-Naphthalimide (1). The reference molecule **1** and its tautomer **1T** in the gas phase in the four solvents and with one, two, and three solvent molecules for each of the solute molecule were studied. In Table 1, the enthalpy and free-energy thermodynamic association functions at 298 K in kilojoules per mole are shown. The most negative values of these functions correspond to the tautomer **1T** in all cases with one, two, or three solvent molecules in their environment. This behavior is particularly interesting for the reactivity and photophysical properties of the molecule because the carbonyl groups favor the intersystem crossing in the excited state, and the imidol form favors a lower state S_1 and more efficient fluorescence emission.[33]

The AcH, followed by *p*-diox, is the solvent with higher negative values for these thermodynamic functions; they can form hydrogen bridge bonds with compound **1** and **1T**. However, DCM and MeCN, with a higher dielectric constant, have similar values for the thermodynamic functions that are lower than those of the AcH and *p*-diox. If we consider one, two, or three molecules around a solute molecule, the relative

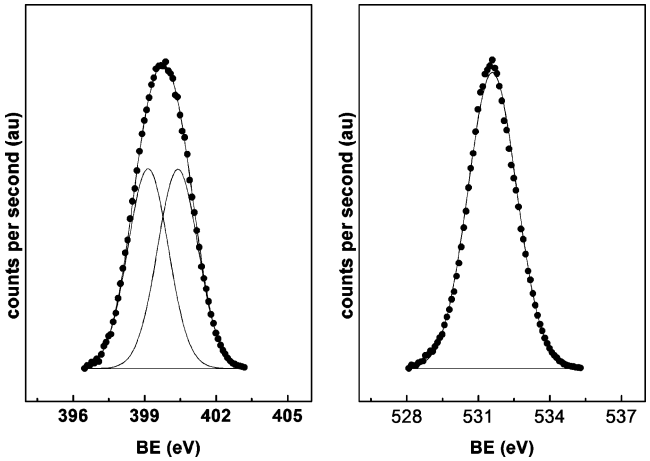

Figure 7. X-ray absorption spectra (vertical axis, arbitrary units) in the regions of binding energies of 396−403 eV (core 1s of imidic nitrogen) and 528−535.5 eV (core 1s of carbonylic oxygen) for a 1,8-naphthalimide solid sample and its decomposition.

TABLE 3: More Probable Rotamers and Tautomers (See Figure 2) Regarding the Absorption Experimental Data for Compounds 2, 3, and 4 for the Gas Phase and *n* Molecules of the Solvent Phase

phase	gas[a]	*p*-diox			AcH			DCM			MeCN		
n		1	2	3	1	2	3	1	2	3	1	2	3
2	Ai	Ao	o	Ao	o	o	o	oT	o	Ao	o	Ao	o
3	o	i	i	o	o	o	o	i	i	o	oT	iT	o
4	t	t	t	t	c	c	c	t	c	t	t	t	t

[a] *p*-Diox as the reference.

variation of these thermodynamic functions in each solvent is small. Table 2 shows the wavelengths (λ) in nanometers and the oscillator strengths (*f*) of the calculated electronic transitions for the more probable structure using both basis sets (6-31G* and cc-pVDZ) and the experimental absorption (λ and log ϵ). We can observe in Table 2 the excellent agreement between experimental and theoretical results. We used both compounds (**1** and **1T**) to study the influence of the basis set. The values of λ and *f* for the 6-31G* and cc-pVDZ basis sets are practically the same, with small variations up to 2 nm and without changes in the relative values of *f*.

Figures 3−6 show the experimental absorption spectra, the calculated transitions for molecules **1** and **1T** in the four solvents, and the optimized geometries of the supermolecule formed by **1** and **1T** and one molecule of solvent. The experimental spectra have a very intense S_2 band with the maximum around 240 nm in *p*-diox, DCM, and MeCN (specific to the naphthalene ring with a chromophore-like electron-withdrawing imide group[34]) and a second S_1 band with two maxima around 330−340 nm associated with the vibrational structure. According to the theoretical transitions calculated in gas phase and in these solvents, the contribution of the tautomer occurs at lower energy and can be associated with the second maxima around 340 nm in the S_1 transition. The XPS of these molecules confirms this contribution (see Figure 7), with the double peak obtained from core IE of N_{1s}. In a previous work,[18] we had considered the double maximum as a vibrational structure, which agrees with the FT−IR study.[35]

It is remarkable that molecule **1** in AcH (see Figure 3) shows an absorption spectrum that is different from the spectra obtained in the other three solvents. The remote UV absorption maximum is displaced 10 nm to the red, and its intensity is very low; the only visible maximum band at approximately 340 nm is wider and more intense than those in the other solvent because of the double bridge bond formed between AcH and the molecule. This interaction modifies their S_1 and S_2 electronic states and favors the tautomeric form in this medium in comparison with a polar solvent like *p*-diox.

From the Mulliken analysis for compound **1** (in gas phase), we can observe that the imidic N charge ($Q_N = -0.70$) is higher than that of any of the carboxyl oxygens ($Q_O = 0.51$). These results agree with core IE of N_{1s} and O_{1s} spectra and previous XPS data.[36] The **1T** molecule breaks the molecular symmetry of molecule **1** (C_{2v}), and consequently, their Q_O (−0.607, −0.480) charge values are different. The asymmetry change in the Q_O in the **1T** compound decreases approximately 0.2e in Q_N (−0.56) due to the increase of Q_O corresponding to C═O and C−OH groups. Q_O charges for compound **1** show that the gas phase has similar values to the ones in *p*-diox and AcH solvents, which can form hydrogen bonds. Q_O and Q_N charges for **1T** in MeCN and DCM show similar values to those obtained in the gas phase, which is supported in the best solvation of a polar solvent with the 1,8-naphthalimide tautomer.

Effects of the Substituents and the Solvents on the N-Substituted 1,8-Naphthalimide Derivatives (2−6). In the theoretical study of the acetamide derivatives (**2** and **3**), we have postulated different conformers (see Figure 2) that present similar energies. However. for the discussion, we only considered the theoretical data of the conformer that show better vertical transition results and whose oscillator strength values have correlation in the UV−vis zones in relation to experimental maxima and extinction coefficient data. In Table 3, we can observe that each solvent produces a different conformer, whose contribution is the most favorable in the electronic transition. In these Table 3, we have selected the corresponding conformer, which is used in the calculation of UV−visible spectra of compounds **2**, **3**, and **4**. Similarly for methoxy derivatives (**4**−

TABLE 4: Calculated ΔH_{as} and ΔG_{as} (kJ/mol at 298 K) Values of 1,8-Naphthalimide Derivatives for *n* Molecules of the Solvent Phase

		2		**3**		**4**		**5**		**6**	
phase	*n*	ΔH_{as}	ΔG_{as}	ΔH_{as}	ΔG_{as}	ΔH_{as}	ΔG_{as}	ΔH_{as}	ΔG_{as}	ΔH_{as}	ΔG_{as}
	1	−21.2	−23.9	−16.4	−20.7	−8.8	−15.3	−10.1	−16.3	−9.7	−16.1
p-diox	2	−12.9	−18.8	−13.3	−20.0	−9.8	−16.8	−9.1	−16.4	−8.8	−15.9
	3	−14.3	−20.8	−9.2	−15.6	−10.3	−17.2	−9.0	−16.1	−8.6	−15.5
	1	−33.5	−35.1	−33.5	−34.3	−22.7	−26.1	−19.8	−22.2	−14.2	−20.5
AcH	2	−23.6	−28.4	−25.0	−28.6	−16.4	−22.3	−18.3	−23.4	−14.9	−21.8
	3	−21.7	−27.8	−22.0	−26.2	−16.7	−23.0	−14.6	−23.0	−18.3	−24.1
	1	−10.6	−16.2	−10.7	−16.0	−10.5	−14.9	−11.7	−16.7	−11.2	−15.6
DCM	2	−10.4	−17.3	−9.9	−17.0	−9.9	−16.3	−9.6	−16.3	−9.7	−16.5
	3	−10.1	−16.5	−9.4	−16.8	−8.9	−15.8	−7.6	−15.1	−8.3	−15.6
	1	−9.8	−15.8	−9.7	−14.3	−8.2	−13.7	−9.5	−14.8	−9.8	−14.3
MeCN	2	−8.9	−15.1	−10.8	−16.7	−8.6	−14.6	−9.0	−15.5	−9.5	−16.2
	3	−10.3	−17.2	−9.8	−17.2	−8.4	−15.1	−9.0	−15.9	−8.8	−16.3

TABLE 5: Theoretical (TD-DFT) Vertical Transitions and UV−Vis Absorption Bands (in nm) of All 1,8-Naphthalimide Derivatives (2−6) for the Gas Phase and *n* Molecules of the Solvent Phase[a]

phase	*n*	2				3				4				5				6			
		λ (nm)	*f*	λ (nm)	log ϵ	λ (nm)	*f*	λ (nm)	log ϵ	λ (nm)	*f*	λ (nm)	log ϵ	λ (nm)	*f*	λ (nm)	log ϵ	λ (nm)	*f*	λ (nm)	log ϵ
gas		366 319 242	0.089 0.081 0.240	–	–	368 243	0.290 0.320	–	–	354 317 233	0.099 0.071 0.214	–	–	348 235	0.231 0.408	–	–	348 235	0.218 0.416	–	–
p-diox	1	376 320 241	0.078 0.108 0.193			375 243	0.288 0.339			356 317 234	0.091 0.100 0.215			350 236	0.222 0.442			350 236 235	0.211 0.288 0.152		
	2	377 324 241	0.080 0.104 0.376	365{381} 324{337} 228{253}	3.730 3.880 4.380	374 243	0.304 0.364	367 248	4.360 4.520	358 319 235	0.094 0.112 0.240	375{361} 331{321} 239{220}	3.318 3.436 3.964	351 237	0.220 0.446	360 240{247}	4.837 5.219	348 235	0.256 0.413	360 240 {247}	4.250 4.683
	3	374 320 240	0.086 0.120 0.264			370 243	0.303 0.390			357 319 235	0.093 0.108 0.198			351 236	0.218 0.461			356 238	0.223 0.421		
AcH	1	369 322 244	0.091 0.106 0.434			363 241	0.335 0.341			384 320 236	0.120 0.091 0.231			352 236	0.227 0.435			347 235	0.243 0.418		
	2	372 324 245	0.089 0.126 0.509	364{374} 340{327} 253{264}	3.723 3.995 4.547	362 240	0.334 0.334	365{348} 251	4.085 4.111	379 320 234	0.140 0.091 0.249	379 336 252	3.854 3.988 4.059	355 237	0.218 0.422	369 252	4.179 4.279	347 235	0.222 0.423	366 251	4.028 4.280
	3	372 323 244	0.096 0.125 0.619			367 241	0.315 0.353			378 320 234	0.129 0.095 0.246			349 236	0.255 0.393			359 237	0.212 0.455		
DCM	1	375 323 263	0.096 0.098 0.547			373 242	0.277 0.329			357 318 235	0.098 0.102 0.211			351 236	0.231 0.409			350 236	0.223 0.436		
	2	370 324 241	0.082 0.122 0.309	366{378} 338 252{230}	4.244 4.508 5.025	373 242	0.298 0.332	365 241	3.776 4.117	382 321 235	0.124 0.086 0.225	378 334 240	4.281 4.392 4.887	354 237	0.230 0.416	364 250	4.121 4.240	354 237	0.224 0.442	364{380} 247{241}	4.138 4.507
	3	378 324 245	0.074 0.118 0.502			370 242	0.328 0.330			386 324 236	0.130 0.081 0.221			355 238	0.233 0.363			358 237	0.232 0.381		
MeCN	1	367 322 239	0.091 0.103 0.335			369 241	0.335 0.367			357 320 235	0.094 0.111 0.210			352 237	0.225 0.419			351 236	0.216 0.447		
	2	373 321 243	0.078 0.106 0.468	378{366} 337{324} 251{227}	3.798 4.073 4.610	369 240	0.372 0.384	364 239 202	4.150 4.481 4.510	361 321 236	0.099 0.119 0.199	376{362} 333{320} 237{221}	3.848 3.982 4.543	357 238	0.225 0.420	362 239{245} 214	4.113 4.440 4.243	356 238	0.216 0.449	362 240{245} 215	4.094 4.468 4.192
	3	376 324 243	0.089 0.131 0.436			371 243	0.318 0.353			361 323 229	0.106 0.118 0.127			360 239 348	0.223 0.427 0.231			359 238 348	0.216 0.448 0.218		

[a] In the brace {} is a submerged band or a less intense band.

6), we have obtained two minimal conformers, cis (c) and trans (t) for the three position derivative (**4**). However, only one minimum (cis) is performed for the four position derivatives (**5** and **6**). We can also observe that the cluster with AcH always produces the same conformers (o for compounds **2** and **3** and c for compound **4**). The differences of energy between the most stable conformer and the other conformers and tautomers are around 2 and 10 kcal/mol, respectively.

Table 4 shows the association of thermodynamic functions (enthalpy and free energy) of the acetamide and methoxy derivatives with one, two, or three molecules in the solvents. These values show similar variations to those of compound **1** in the respective solvents. The AcH, followed by *p*-dioxane, has the most negative values of the thermodynamic association functions with the acetamide derivatives **2** and **3**, and DCM and MeCN have the least negative values. The different conformers can form some hydrogen bridge bond with the AcH and *p*-dioxane solvent and electrostatic interactions with the DCM and MeCN. An entropic factor contributes to the more negative value of the thermodynamic function, which favors the supermolecular structure formation between the acetamide derivatives and the solvents studied.

The methoxy derivatives **4**−**6** have more negative values of the thermodynamic functions in AcH because they can form hydrogen bridge bonds in this solvent. These derivatives in *p*-diox, DCM, and MeCN give similar values because the interactions with the solvent molecules are only of the electrostatic kind. The importance of the hydrogen bond formation between these molecules and the porous silicon surface has been observed using FT−IR spectroscopy. Moreover, the photoluminescence properties of the crystal obtained by deposition of compounds **3** and **5** on nanostructured porous silicon have been measured.[37]

In regards to the number of solvent molecules around the solute molecule, in Table 4, we can observe for the MeCN solvent that ΔG increases the negative value when the solute molecule has 1−3 solvent molecules. This solvent has a higher dielectric constant and forms a more stable cage around the solute molecule than the other solvents because of the electrostatic interactions. This could explain the stabilization of the polar molecular forms in this solvent, which in the excited-state, favor the intramolecular charge transfer (ICT) observed in the experimental study for **3**, **5**, and **6** derivatives.[19]

Table 5 shows the wavelength (nm) and the oscillator strength of the molecular electronic transitions calculated with TD-DFT methods and the experimental absorption transition. The **3** (4-acetamide), **5**, and **6** (4-methoxy) compounds have an UV band S_2 around 250 nm and a visible and wide band S_1 around 365 and 360 nm, respectively. The **2** (3-acetamide) and **4** (3-methoxy) compounds have a similar band in the UV; in the visible zone, and a band which is the same as that of compound **1** and an additional band more red-shifted at 375 and 380 nm (new S_1) appears. This spectroscopic behavior is reproduced by the theoretical data, although the experimental band of compounds **5** and **6** at 360 nm is reproduced at 350 nm, 10 nm displaced to the blue (see Figures S4 and S5). According to the high values of the oscillator strength of the UV band, we can consider that the transitions are of the $\pi-\pi^*$ type, although in the visible band, they are mixed with the $n-\pi^*$ type. UV−visible spectra corresponding to these five derivatives in the four solvents are depicted in the Supporting Information (Figures S1−S5). In each Figure, the four spectra for each derivative, including an inset of the theoretical vertical transition and a scheme of the derivative and its interaction with a solvent molecule, are shown. A general inspection of the Supporting Information shows the excellent agreement between experimental and theoretical spectra. It is remarkable that the maxima corresponding to the UV−visible spectra are very well reproduced by theoretical methodology, that is, compound **3** in MeCN (see Figure S2) and compound **4** in *p*-diox (see Figure S3).

TABLE 6: Distances from the Heteroatom of R_2 to the Nearest Aromatic Carbon (in Å) in the Gas Phase and with One Molecule of Solvent in the AM1-Optimized Geometries

phase	2	3	4	5	6
Gas	1.403(Ai)	1.398(o)	1.381(t)	1.376	1.376
p-diox	1.403(Ao)	1.397(i)	1.381(t)	1.376	1.376
AcH	1.406(o)	1.399(o)	1.380(c)	1.376	1.375
DCM	1.405(oT)	1.399(i)	1.380(t)	1.375	1.375
MeCN	1.406(o)	1.400(oT)	1.381(t)	1.375	1.375

Table 6 shows the distances from the heteroatom of R_2 to the aromatic C for the derivatives **2**−**6** with one molecule of the different solvents in the AM1-optimized geometries. If we analyze the trends between the distances of **4** (3-methoxy) and **5** and **6** (4-methoxy), we observe that the three position has longer distances than those of the four position, and this group is nearly coplanar to the rings of the molecule. Regarding the distances, the compounds **2** and **3** of the R_2 group with respect to the C of the naphthalene ring have similar behavior, but this group is not coplanar with respect to the rings due to steric effects. Shorter distances favor the charge transfer of the R_2 group to the chromophore formed by the naphthalene ring and the carboximide group. This behavior agrees with the spectroscopic band in the visible zone, with only one maximum for the derivatives substituted in the four position and with two maxima for the derivatives substituted in the three position.

All derivatives **2**−**6** present a Q_N value around −0.54, whereas the compound **1** has a value of approximately −0.71 in the gas phase. In the meantime, in all derivatives, the Q_O values are higher (0.52−0.53) than that in compound **1** (0.50−0.51). These values in the solvent medium show the same tendency. This implies that the N imide-carbonyl group bond decreases its polar character in all derivatives **2**−**6** with respect to the farther molecule **1** and contributes to the other different polar forms of the tautomerism. The heteroatom charges (Q_X) of the $R_2 = -$(N)-HCOMe group in compounds **2** and **3** are higher than those of **4**, **5**, and **6** for all phases. These results agree with the semireduction redox potentials obtained in our laboratory by means of cyclic voltammetry,[18,38] which indicates that the acetamide group has lower electronic-donating character in the fundamental state than the methoxy group. The heteroatom charges of $R_2 = -$(O)-Me are independent of the R_1 substituent since $Q_X \sim 0.51-0.52$ are very similar in the three and four positions of $R_2 = -$(O)-Me for compounds **4**−**6**. Nevertheless, compounds **5** and **6** show similar experimental absorption spectra, and the spectra of compound **4** are different, with three absorption bands.

Conclusions

The experimental absorption UV−visible spectra for the six compounds in the four solvents were obtained in our laboratory, and XPS of the 1,8-naphthalimide was carried out in the ICP−CSIC laboratory. We have computed the theoretical spectra of the six compounds using TD-DFT in gas phase and with one, two, or three solvent molecules in their environment. For this study, three aprotic solvents with different polarity (MeCN, *p*-diox, and DCM) were selected. A protic and polar solvent such as AcH was also considered because this acid has been employed to eliminate the ICT effect. The absorption spectra

were compared with the theoretical electronic transition results, considering the interaction between the different conformations of these molecules with the four solvents. Furthermore, thermodynamic association function values of these naphthalimide derivatives were obtained. These results show the higher association energies in the clusters of the solvents that can form hydrogen bridge bonds.

The main interest of this paper is the feasibility of a way for calculating with theoretical methods the possible contribution of conformers and tautomers to the electronic transitions in solution with different solvents. The thermodynamic association function values computed in this paper have a good correlation with the kind and the position of the substituent and with the solvent considered. The electronic transition values and their oscillator strengths obtained with TD-DFT (B3LYP/6-31G*) agree with the experimental absorption bands obtained by us for the six molecules in three solvents (DCM, MeCN, and *p*-diox), particularly for compounds **1** and **4**−**6**.

The highest associations of solute−solvent molecules are shown in AcH and partially in *p*-diox. These solvents have the highest proton-donating and proton-accepting character, respectively. Furthermore, substituents with the acetamide group in R_2 (compounds **2** and **3**) have the most negative ΔG values, which indicate its highest interaction ability with all solvents. The more stable solvent cage is obtained with three solvent molecules for MeCN, the most polar solvent.

Other theoretical parameters considered in this work, such as the interatomic distances and atomic charges, agree with the experimental properties observed. From these data, the imide−imidol tautomerism is considered. Imide−imidol forms (R′−NH−C(=O)−R ↔ R′−N=C(OH)−R) contribute to the electronic transition depending on the solvent. XPS, reported in this paper, confirms this tautomerism.

This work is a step toward a more extensive application of computational chemistry in order to clarify the experimental behavior of the organic molecules in solution and their photophysical properties.

Acknowledgment. This paper is dedicated to the memory of Professor Antonio Pardo for his contribution to the spectroscopy of 1,8-naphthalimide derivatives. The authors acknowledge the computational support of the UAM Centro de Computación Científica. The financial support from Ministerio de Ciencia y Tecnología by the projects BQU2002/01502, CTQ2004/6615, and CTQ2007/63332 is gratefully acknowledged.

Supporting Information Available: Experimental and theoretical UV spectra of compounds **2**−**6** in the four solvents and the corresponding minimum geometries for the interaction compound with one solvent molecule. This material is available free of charge via the Internet at http://pubs.acs.org.

References and Notes

(1) Stewart, W. W. *Nature* **1981**, *292*, 17.
(2) Martín, E.; Weigand, R.; Pardo, A. *J. Lumin*. **1996**, *68*, 157.
(3) Constantinova, T.; Grachev, I. *Polym. Int*. **1997**, *43*, 39.
(4) Gan, J. A.; Tian, H.; Chen, K. C. *Polym. Adv. Technol*. **2002**, *13*, 584.
(5) Ramachandram, B.; Sankaran, N. B.; Karmakar, R.; Saha, S.; Samantha, A. *Tetrahedron* **2000**, *56*, 7041.
(6) Grabchev, I.; Quian, X. H.; Xiao, Y.; Zhang, R. *New J. Chem.* **2002**, *26*, 920.
(7) Guo, X.; Qian, X.; Jia, L. *J. Am. Chem. Soc*. **2004**, *126*, 2272.
(8) Xu, Z.; Quian, X.; Cui, J. *Org. Lett*. **2005**, *7*, 3029.
(9) Yin, S.; Liu, X.; Li, C.; Huang, W.; Li, W.; He, B. *Thin Solid Films* **1998**, *325*, 268.
(10) Kolosov, D.; Adamovich, V.; Djurovich, P.; Thompson, M. E.; Adachi, C. *J. Am. Chem. Soc.* **2002**, *124*, 9945.
(11) Braña, M. F.; Castellano, J. M.; Roldan, C. M.; Santos, A.; Vazquez, D.; Jiménez, A. *Cancer Chemother. Pharmacol*. **1980**, *4*, 61.
(12) Rogers, J. E.; Abraham, B.; Rostkowski, A.; Kelly, L. A. *Photochem. Photobiol*. **2001**, *74*, 521.
(13) Li, Z.; Yang, Q.; Qian, X. *Bioorg. Med. Chem. Lett*. **2005**, *15*, 3143.
(14) Yang, Q.; Xu, J.; Sun, Y.; Li, Z.; Li, Y.; Qian, X. *Bioorg. Med. Chem. Lett*. **2006**, *16*, 803.
(15) Pardo, A.; Poyato, J. M. L.; Martín, E. *J. Photochem.* **1987**, *36*, 323.
(16) Pardo, A.; Poyato, J. M. L.; Martín, E.; Camacho, J. J.; Reyman, D.; Braña, M. F.; Castellano, J. M. *J. Photochem. Photobiol., A* **1989**, *46*, 323.
(17) Martín, E.; Coronado, J. L. G.; Pardo, A.; Camacho, J. J. *Opt. Pura Apl*. **2004**, *37*, 65.
(18) Martín, E.; Coronado, J. L. G.; Camacho, J. J.; Pardo, A. *J. Photochem. Photobiol., A* **2005**, *175*, 1.
(19) Pardo, A.; Martín, E.; Poyato, J. M. L.; Camacho, J. J.; Guerra, J. M.; Weigand, R.; Braña, J. M. F.; Castellano, J. M. *J. Photochem. Photobiol., A* **1989**, *48*, 259.
(20) Xiao, Y.; Liu, F.; Quian, X.; Cui, J. *Chem. Commun*. **2005**, 239.
(21) Pardo, A.; Reyman, D.; Poyato, J. M. L.; Camacho, J. J.; Martín, E. *J. Mol. Struct.:THEOCHEM* **1988**, *166*, 463.
(22) Patsenker, L. D.; Artyukhova, T. T. *J. Mol. Struct.* **2003**, *655*, 311.
(23) de la Peña O'shea, V. A.; Pardo, A.; Poyato, J. M. L. *Int. J. Quantum Chem.* **2003**, *91*, 446.
(24) Montero, L. A.; Esteva, A. M.; Molina, J.; Zapardiel, A.; Hernandez, L.; Marquez, H.; Acosta, A. *J. Am. Chem. Soc.* **1998**, *120*, 12023.
(25) Stewart, J. J. P. *MOPAC, A Semi-Empirical Molecular Orbital Program*, QCPE, Program No. 455 Version 6.0, 1993.
(26) Codorniu-Hernandez, E.; Mesa-Ibirico, A.; Montero-Cabrera, L.; Martinez-Luzardo, F.; Stohrer, W. D. *J. Mol. Struct.:THEOCHEM* **2005**, *715*, 227.
(27) Montero, L. A.; Molina, J.; Fabian, J. *Int. J. Quantum Chem.* **2000**, *79*, 8.
(28) Casida, M. E. In *Recent Advances in Density Functional Methods, Part 1*; Chong, D.P., Ed.; World Scientific: Singapore, 1995.
(29) (a) Casida, M. E.; Jamorski, C.; Casida, K. C.; Salahub, D. R. *J. Chem. Phys.* **1998**, *108*, 4439. (b) Stratmann, R. E.; Scuseria, G. E.; Frisch, M. J. *J. Chem. Phys.* **1998**, *109*, 8218.
(30) (a) Becke, A. D. *J. Chem. Phys.* **1993**, *98*, 1372. (b) Becke, A. D. *J. Chem. Phys.* **1993**, *98*, 5648.
(31) Lee, C.; Yang, W.; Parr, R. G. *Phys. Rev. B* **1988**, *37*, 785.
(32) Frisch, M. J.; Trucks, G. W.; Schlegel, H. B.; Scuseria, G. E.; Robb, M. A.; Cheeseman, J. R.; Montgomery, J. A., Jr.; Vreven, T.; Kudin, K. N.; Burant, J. C.; Millam, J. M.; Iyengar, S. S.; Tomasi, J.; Barone, V.; Mennucci, B.; Cossi, M.; Scalmani, G.; Rega, N.; Petersson, G. A.; Nakatsuji, H.; Hada, M.; Ehara, M.; Toyota, K.; Fukuda, R.; Hasegawa, J.; Ishida, M.; Nakajima, T.; Honda, Y.; Kitao, O.; Nakai, H.; Klene, M.; Li, X.; Knox, J. E.; Hratchian, H. P.; Cross, J. B.; Bakken, V.; Adamo, C.; Jaramillo, J.; Gomperts, R.; Stratmann, R. E.; Yazyev, O.; Austin, A. J.; Cammi, R.; Pomelli, C.; Ochterski, J. W.; Ayala, P. Y.; Morokuma, K.; Voth, G. A.; Salvador, P.; Dannenberg, J. J.; Zakrzewski, V. G.; Dapprich, S.; Daniels, A. D.; Strain, M. C.; Farkas, O.; Malick, D. K.; Rabuck, A. D.; Raghavachari, K.; Foresman, J. B.; Ortiz, J. V.; Cui, Q.; Baboul, A. G.; Clifford, S.; Cioslowski, J.; Stefanov, B. B.; Liu, G.; Liashenko, A.; Piskorz, P.; Komaromi, I.; Martin, R. L.; Fox, D. J.; Keith, T.; Al-Laham, M. A.; Peng, C. Y.; Nanayakkara, A.; Challacombe, M.; Gill, P. M. W.; Johnson, B.; Chen, W.; Wong, M. W.; Gonzalez, C.; Pople, J. A. *Gaussian 03*, revision C.02; Gaussian, Inc.: Pittsburgh, PA, 2004.
(33) Turro, N. J. *Modern Molecular Photochemistry*; University Science Books: Sausalito, CA, 1991; p 153.
(34) Gawronski, J.; Gawronska, K.; Skowronek, P.; Holmen, A. *J. Org. Chem.* **1999**, *64*, 234.
(35) Philiphova, T.; Karamancheva, I.; Grabchev, I. *Dyes Pigm.* **1995**, *28*, 91.
(36) Bigotto, A.; Galasso, V.; Distefano, G.; Modelli, A. *J. Chem. Soc., Perkin Trans. 2* **1979**, 1502.
(37) Martín, E.; Torres-Costa, V.; Martín-Palma, R. J.; Bousoño, C.; Tutor-Sandres, J.; Martínez-Duart, J. M. *J. Electrochem. Soc.* **2006**, *153*, 1.
(38) Martín, E.; Weigand, R. *Chem. Phys. Lett.* **1998**, *288*, 52.